SAND2016-9288J

# The Initial Pump-Probe Polarization Anisotropy of Colloidal PbS Quantum Dots

**Samuel D. Park, Dmitry Baranov, Jisu Ryu, and David M. Jonas**
*Department of Chemistry and Biochemistry, University of Colorado, 215 UCB, Boulder, CO 80309, USA*
*e-mail: david.jonas@colorado.edu*

**Abstract:** Pump-probe polarization anisotropy measurements with 15 fs pulses are employed to investigate the electronic structure of PbS quantum dots. The initial anisotropy at the bandgap is anomalously low (<0.1) and suggests large electronic couplings.
**OCIS codes:** 320.7130 (Ultrafast processes in condensed matter); 300.6290 (Spectroscopy, four-wave mixing)

## 1. Introduction

Bulk lead chalcogenide semiconductors have a rock salt structure and an interesting electronic structure, with their bandgap at the 4-fold degenerate (8-fold including spin) L-point of the first Brillouin zone, where $\vec{k} = (\pm\pi/a, \pm\pi/a, \pm\pi/a)$ [1]. The four L-points in the band structure are each local minima in the conduction band, and local maxima in the valence band, which are known as valleys. The electronic structure near the bandgap of their quantum dots (QDs) is more complicated than suggested by the particle in a sphere model commonly used to explain quantum confinement [2]. Theoretical studies report that the splittings of the energy levels in lead chalcogenide QDs due to intervalley coupling are sensitive to the arrangement of atoms having an inversion center, stoichiometry of the QDs, and the surface passivation [3]. If correct, the predicted variation in splitting with structural details either implies nanostructures of unprecedented uniformity or casts doubt on the experimental attribution. The theoretical results imply that the confinement gives rise to a complex electronic structure, which affects both linear and non-linear spectroscopic measurements.

The pump-probe polarization anisotropy is a valuable technique for probing the electronic structure of QDs. The anisotropy can provide structural information on the angles between transition dipoles. In an orientationally isotropic ensemble of molecules with non-degenerate transitions, the initial anisotropy should be 2/5, because the $\cos^2(\theta)$ dipolar excitation probability gives rise to a 3:1 signal strength ratio between parallel and perpendicular polarization geometries.

Rosenthal et al. [4], using 10 fs pulses, reported initial anisotropies of 0.1 to 0.4 for CdSe QDs. The anisotropy decreased as the diameter of the QD increased and the QDs became more spherical. Rosenthal et al. [4] attributed the anisotropy to a change in the symmetry and degeneracy of the conduction and valence orbitals with change in QD size. This interpretation of the anisotropy is incomplete, because it did not consider the different anisotropies of the ground state bleach and excited state absorption, which were first treated in later work [5]. This later work predicts that even in the high symmetry structure the coherent initial anisotropy is always 2/5 so long as pulses capture all coupled single excitations. Fundamentally, this is a property of dipolar excitation by a linearly polarized optical field.

In this work, spectrally resolved pump-probe (SRPP) polarization anisotropy measurements with 15 fs pulse durations are employed to investigate the electronic structure of chlorine-passivated lead sulfide (PbS) QDs at the bandgap. The measurement of the initial anisotropy required the removal of unwanted signal contribution from cross-phase modulation (XPM). The initial anisotropy contains information about both bi-exciton states and some hot single exciton states, and the time dependence quantifies the timescale of intervalley scattering. Our results for PbS QDs indicate an anomalously lower initial anisotropy than expected from an effective mass approximation for PbS QDs with a rapid loss of any anisotropy in less than 10 fs.

## 2. Experimental Methods

Pulses from a 1 kHz Ti:Sapphire regenerative amplifier pump a single-pass, short-wave IR non-collinear optical parametric amplifier with a PPSLT crystal [6]. The pulses are compressed with a deformable mirror using SHG feedback in a genetic algorithm, to pulse durations of 15 fs. The pulse spectrum is centered at 1.04 eV, and has a FWHM of ~240 meV. Pulses at the sample position are characterized using SHG FROG with the corrections for broad bandwidth pulses given by Baltuska et al. [7]. The FROG trace is reconstructed down to the 0.3% contour and the independently measured pulse spectrum is accurately retrieved by FROG. The spectrum and phase enable accurate simulation of experimentally measured XPM in solvent/glass. Nonlinear optical experiments on the sample of PbS QDs (with a bandgap of 1.074 eV and FWHM of the first exciton peak of 101 meV) were performed using a custom built UHV-compatible spinning sample cell [8].

## 3. Results and Discussion

The SRPP signal at early times (during pulse overlap) is dominated by XPM originating from solvent/glass [9]. The XPM signal is proportional to the square of the peak intensity, and therefore, becomes more apparent with shorter pulses. Because the initial anisotropy contains information about the bi-exciton states, an XPM subtraction scheme is used to reveal the dynamics of the PbS QDs during pulse overlap [10]. The XPM signal can be simulated assuming a delta function response with the pulse phase and amplitude retrieved from FROG. Fig. 1a and Fig. 1b show the comparison between the experimentally measured and simulated XPM SRPP transient, respectively. The simulation shows agreement with the measured XPM within 10%.

As a check on the polarized measurements, the SRPP XPM signal from solvent/glass was detected with both parallel and perpendicular polarization geometries. Fig. 1c shows the anisotropy as a function of frequency taken at different time delays from the XPM SRPP transients. The anisotropy of the XPM where there is signal is ~2/5, which is consistent with previous reports on the signal strength ratio of 3:1 in XPM with parallel and perpendicular polarization geometries [11]. For each delay, the anisotropy diverges in regions where there is no XPM signal.

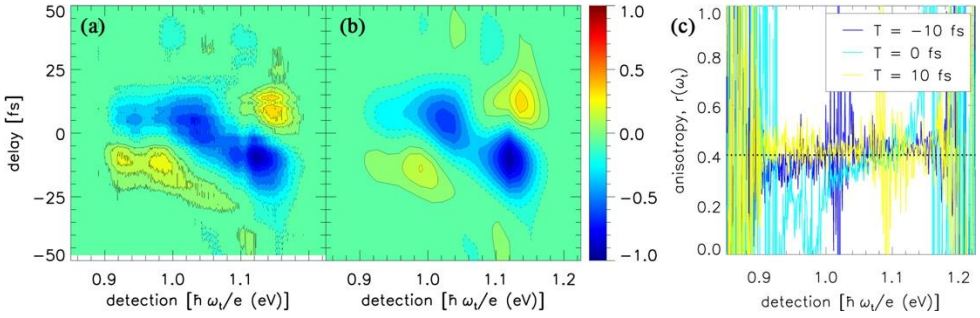


**Fig. 1** Experimental **(a)** and simulated **(b)** spectrally resolved pump-probe XPM from sample windows and neat solvent. The XPM signal was simulated with the retrieved pulse spectrum and spectral phase from FROG. The simulation shows agreement with the measured XPM within 10%. **(c)** Anisotropy of glass from XPM. The XPM signal strength has the expected 3 to 1 ratio between parallel and perpendicular polarization geometries, which results in an anisotropy of 2/5. For each delay, the anisotropy diverges around sign changes in the XPM.

The XPM was calculated including absorptive and dispersive propagation effects to account for pulse attenuation from absorption by the QDs [12]. The calculation was used to determine a multiplicative scale factor for subtraction of experimentally measured XPM SRPP transients from the SRPP transients with both QDs and solvent/glass. For this sample with an optical density of 0.3 at the first exciton peak and a sample pathlength of 270 microns, the multiplicative factor for XPM in neat solvent for subtraction is 0.53. After subtraction of XPM, the parallel and perpendicular polarization geometry SRPP transients for the PbS QDs are revealed. Fig. 2a and Fig. 2b show the SRPP transient for PbS QDs for parallel and perpendicular polarization geometries, respectively. Fig. 2c shows the signal near the bandgap and the calculated anisotropy. Our result shows a nominally zero anisotropy, but may be compatible with a small initial anisotropy of up to ~0.1.

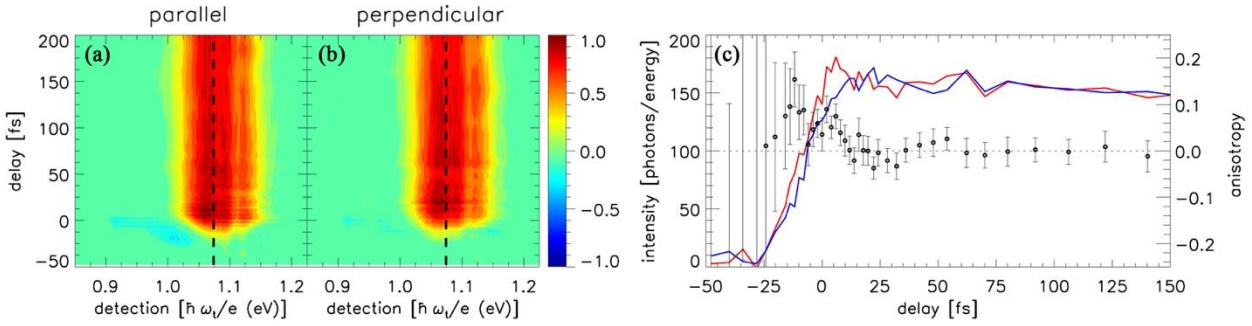


**Fig. 2** PbS anisotropy at the bandgap. SRPP signal for PbS QDs after the XPM subtraction with the parallel **(a)** and perpendicular **(b)** polarization geometries. **(c)** Anisotropy slice near the bandgap (1.074 eV), shown as the black vertical dashed line in panels **(a)** and **(b)**, for the parallel (red) and perpendicular (blue) polarization geometries. The black circles show the calculated anisotropy with error bars from laser fluctuations as a function of time delay. The anisotropy diverges where there is no signal.

Fig. 3 shows the anisotropy as a function of the detection frequency at different time delays, *T*. The black dashed line in Fig. 3 shows the linear absorption spectrum. The anisotropy diverges where there is no signal, which is all outside of the first exciton peak. In addition, the anisotropy as a function of the detection energy shows that there is

no contribution from the red-shifted photoluminescence spectrum. This is consistent with the hypothesis that the red-shifted photoluminescence signal arises from lower fine structure states with long radiative lifetimes. Such states would not be populated immediately after excitation and would have low stimulated emission cross sections [13].

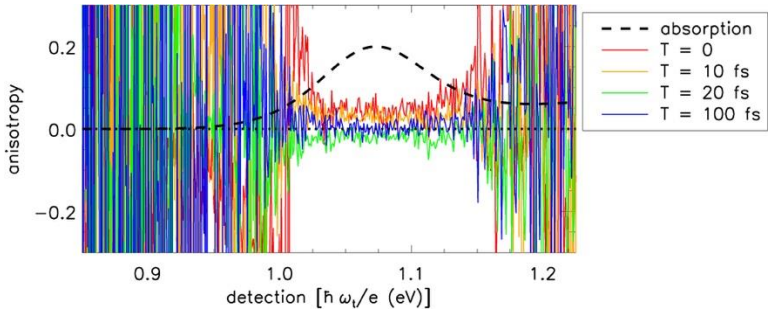


**Fig. 3** PbS anisotropy as a function of the detection frequency in energy at variable *T* delays. The black dashed line represents the linear absorption spectrum and the black dotted line denotes zero. The different colors show the anisotropy at different delays and labeled in the legend.

The initial anisotropy we report for PbS QDs at the bandgap is nominally zero, which is anomalous and suggests coupling to singly excited states outside the ~240 meV pulse bandwidth on a timescale very much less than 15 fs pulse duration. The fastest dephasing time allowed by the width of the first exciton peak is ~8 fs, meaning the initial dynamics should have been captured at least partially with the time resolution in the experiment. Calculation using an effective mass approximation yields an initial anisotropy of 2/5 so long as all intervalley splittings and bi-exciton binding shifts remain within the pulse spectrum. Theoretical studies have predicted splittings from intervalley coupling less than 80 meV for lead selenide (PbSe) QDs [14]. Strong spin-orbit coupling or strong excited state absorption to hot one-electron states might lower the initial anisotropy. To explain the initial anisotropy, couplings much larger than all theoretical predictions are needed to push some of these states outside of our pulse bandwidth.

## Acknowledgements

This work was funded by the Division of Chemical Sciences, Geosciences, and Biosciences, Office of Basic Energy Sciences of the U.S. Department of Energy through Grant DE-FG02-07ER15912.

## References

1. Y. I. Ravich, B. A. Efimova, and I. A. Smirnov, *Semiconducting lead chalcogenides* (Plenum Press, 1970).
2. A. L. Efros, and A. L. Efros, "Interband Absorption of Light in a Semiconductor Sphere," Sov Phys Semicond **16**, 772-775 (1982).
3. A. N. Poddubny, M. O. Nestoklon, and S. V. Goupalov, "Anomalous suppression of valley splittings in lead salt nanocrystals without inversion center," Phys Rev B **86** (2012).
4. S. J. Rosenthal, A. T. Yeh, A. P. Alivisatos, and C. V. Shank, "Size Dependent Absorption Anisotropy Measurements of CdSe Nanocrystals: Symmetry Assignments for the Lowest Electronic States," in *Ultrafast Phenomena X: Proceedings of the 10th International Conference, Del Coronado, CA, May 28 – June 1, 1996*, P. F. Barbara, J. G. Fujimoto, W. H. Knox, and W. Zinth, eds. (Springer Berlin Heidelberg, 1996), pp. 431-432.
5. A. A. Ferro, and D. M. Jonas, "Pump-probe polarization anisotropy study of doubly degenerate electronic reorientation in silicon naphthalocyanine," J Chem Phys **115**, 6281-6284 (2001).
6. D. Brida, S. Bonora, C. Manzoni, M. Marangoni, P. Villoresi, S. De Silvestri, and G. Cerullo, "Generation of 8.5-fs pulses at 1.3 mu m for ultrabroadband pump-probe spectroscopy," Opt Express **17**, 12510-12515 (2009).
7. A. Baltuska, M. S. Pshenichnikov, and D. A. Wiersma, "Second-harmonic generation frequency-resolved optical gating in the single-cycle regime," Ieee J Quantum Elect **35**, 459-478 (1999).
8. D. Baranov, R. J. Hill, J. Ryu, S. D. Park, and D. M. Jonas, (In preparation).
9. R. Trebino, K. W. DeLong, D. N. Fittinghoff, J. N. Sweetser, M. A. Krumbugel, B. A. Richman, and D. J. Kane, "Measuring ultrashort laser pulses in the time-frequency domain using frequency-resolved optical gating," Rev Sci Instrum **68**, 3277-3295 (1997).
10. S. Dong, D. Trivedi, S. Chakrabortty, T. Kobayashi, Y. Chan, O. V. Prezhdo, and Z. H. Loh, "Observation of an Excitonic Quantum Coherence in CdSe Nanocrystals," Nano Lett **15**, 6875-6882 (2015).
11. Q. Lin, and G. P. Agrawal, "Vector theory of cross-phase modulation: Role of nonlinear polarization rotation," Ieee J Quantum Elect **40**, 958-964 (2004).
12. M. K. Yetzbacher, N. Belabas, K. A. Kitney, and D. M. Jonas, "Propagation, beam geometry, and detection distortions of peak shapes in two-dimensional Fourier transform spectra," J Chem Phys **126** (2007).
13. M. Nirmal, D. J. Norris, M. Kuno, M. G. Bawendi, A. L. Efros, and M. Rosen, "Observation of the Dark Exciton in Cdse Quantum Dots," Phys Rev Lett **75**, 3728-3731 (1995).
14. J. M. An, A. Franceschetti, and A. Zunger, "The excitonic exchange splitting and radiative lifetime in PbSe quantum dots," Nano Lett **7**, 2129-2135 (2007).